ELSEVIER

Materials Science and Engineering B96 (2002) 145–149

MATERIALS SCIENCE & ENGINEERING B

www.elsevier.com/locate/mseb

Local atomic arrangement of Pb and Sn on the Si(111)$\sqrt{3} \times \sqrt{3}$-(Pb,Sn) surface

J. Yuhara [a,*], T. Takada [a], D. Nakamura [a,1], K. Soda [a], M. Kamada [b]

[a] Department of Crystalline Materials Science, Graduate School of Engineering, Nagoya University, Furo-cho, Chikusa-ku, Nagoya 464-8603, Japan
[b] UVSOR, Institute for Molecular Science, Myodaiji, Okazaki 444-8585, Japan

Abstract

A $\sqrt{3} \times \sqrt{3}$-(Pb,Sn) surface was studied by means of scanning tunneling microscopy (STM) and core-level photoelectron spectroscopy (PES) to identify its local atomic arrangement. Observed spots in STM were classified into three types, which were white and gray (α), gray and white (β), and black and gray (γ) spots in the filled- and empty-state images, respectively. The STM images also showed a local 3 × 3-(Pb,Sn) arrangement in the $\sqrt{3} \times \sqrt{3}$-(Pb,Sn) surface. Both Pb 5*d* and Sn 4*d* core-levels spectra indicated that there were two components on the $\sqrt{3} \times \sqrt{3}$-(Pb,Sn) surface, and the peak positions and shapes of Pb 5*d* and Sn 4*d* core-levels of the $\sqrt{3} \times \sqrt{3}$-(Pb,Sn) surface were almost the same as those of the $\sqrt{3} \times \sqrt{3}$-Pb and $\sqrt{3} \times \sqrt{3}$-Sn surfaces. Comparison between the heights of the STM spots on the single and binary adsorbate surfaces and their core-levels spectra suggested that Sn and Pb were located at α and β positions, respectively. The nominal coverage of the local 3 × 3-(Pb,Sn) arrangement was determined to be 1/9 and 2/9 ml for Sn and Pb, respectively. © 2002 Elsevier Science B.V. All rights reserved.

Keywords: Scanning tunneling microscopy; Photoelectron spectroscopy; Atomic arrangement; Chemical shift; Silicon; Lead; Tin

1. Introduction

The basic understanding of metal-semiconductor interfaces is important from not only a purely scientific point of view but also technological development. The Pb/Si(111) and Sn/Si(111) systems are considered to be a model system for an unreactive interface due to the negligible mutual bulk solubility [1]. In both systems, annealing of a Si(111) substrate deposited with 1/3 ml (1 ml for the Si(111) face $= 7.8 \times 10^{14}$ atoms cm^{-2}) coverage of Pb or Sn leads to a $\sqrt{3} \times \sqrt{3}$ reconstruction surface [2,3], where both Pb and Sn are located at the T4 site [2,4]. When the coverage of Pb or Sn decreases to 1/6 ml, both the $\sqrt{3} \times \sqrt{3}$ phases change into $\sqrt{3} \times \sqrt{3}$ mosaic phases, which consist of alternating chains of Pb (Sn) and Si adatoms in the T4 site with 1:1 Pb (Sn) to Si ratio [2,3]. Thus, the atomic arrangement of Pb in a thin layer on the Si(111) surface is very much similar to that of Sn.

Recently, great attention has been focused on the understanding of atomic arrangement and electronic structure of binary adsorbates on the semiconductor surface to control crystalline growth mode, such as perfect flat interface and nano-dots [5,6]. In the case of (Pb,Sn) binary adsorbates on the Si(111) surface, they form unique $2\sqrt{7} \times 3$ and $\sqrt{7} \times \sqrt{3}$ structures at the total coverage of $0.7 \sim 0.8$ ml [7–9], although they are immiscible in bulk. We have also observed that co-adsorbates of Pb and Sn form a $\sqrt{3} \times \sqrt{3}$ reconstruction at the total coverage of 1/3 ml. Therefore, it is interesting to study local atomic arrangements and electronic structures of (Pb,Sn) co-adsorbates at low coverage on the Si(111) surface.

In this paper, the Si(111)$\sqrt{3} \times \sqrt{3}$-(Pb,Sn) surface at single and binary adsorbates have been studied by topographic scanning tunneling microscopy (STM) and Pb 5*d* and Sn 4*d* core-level photoelectron spectroscopy (PES) in order to discriminate the adsorbate

---

* Corresponding author. Tel.: +81-52-789-3604; fax: +81-52-789-5155

E-mail address: j-yuhara@nucl.nagoya-u.ac.jp (J. Yuhara).

[1] Present address: Toyota Central R&D Labs., Inc. Nagakute-cho, Aichi-gun, Aichi, 480-1131, Japan.

PII: S0921-5107(02)00306-9

elements on the STM images and identify the local atomic arrangement. It will be shown that Pb and Sn form a local 3 × 3 reconstruction and that the local bondings of Pb and Sn for the binary adsorbate system are almost the same as those for the single adsorbate system.

2. Experimental

Specimens were mirror-polished n-type Si(111) wafers with a resistivity of 3 Ωcm in sizes of $15 \times 3 \times 0.5$ and $15 \times 6 \times 0.5$ mm^3 for STM and core-level PES measurements, respectively. In the STM measurement, the specimen was placed on a manipulator under 1×10^{-8} Pa base pressure in a conventional UHV chamber that consisted of a commercial STM (UNISOKU-USM800) vessel and a low energy electron diffraction (LEED) optics with two evaporation sources for Pb and Sn. All the STM images were obtained at tip biases up to ±1.0 V and the tunneling current of 0.2 nA in a topographic mode. Core-level PES experiments were performed at beamline 5 A of a 0.75 GeV electron storage ring UVSOR at the Institute for Molecular Science. In the PES measurement, the specimen was placed on a manipulator under 5×10^{-9} Pa base pressure in the UHV chamber equipped with a LEED optics, a hemispherical electron energy analyzer ($\Delta E = 0.04$ eV) with an angular acceptance of ±8° at the normal emission angle, and two evaporation sources for Pb and Sn. Excitation photon energy of 52 eV was used at the 45° incident angle in this study. The energy spread of excitation photon was 0.04 eV. The binding energy was determined from the Fermi edge of a Ta plate that holds the Si wafer. The total energy resolution was estimated to be about 0.10 eV from the Ta Fermi edge.

The substrate surface was cleaned by repeated direct current heating for 5 min at no less than 1050 °C at pressures below 2×10^{-7} Pa. After the cleaning process, a distinct 7 × 7 LEED pattern was observed. The binary metal adsorbates of Pb and Sn on the Si(111) surface were prepared by their deposition and subsequent thermal annealing in turn. Sn films of 1/6 ml were deposited onto the Si(111)-7 × 7 surface at RT and annealed at 550 °C for 5 min to form a mixed domains of the $\sqrt{3} \times \sqrt{3}$-Sn and 7 × 7. Then, Pb films of 1/6 ml were deposited onto the a mixed domains of the $\sqrt{3} \times \sqrt{3}$-Sn and 7 × 7 and annealed at a temperature of 300 °C for 2 min to form a Si(111)$\sqrt{3} \times \sqrt{3}$-(Pb,Sn) surface, which was confirmed by LEED observation. Since thickness of Pb and Sn deposited could not be measured directly, they were monitored by a quartz oscillator, which were calibrated with ex-situ Rutherford backscattering spectrometry (RBS) measurements.

3. Results and discussion

Typical topographic STM images of the Si(111)$\sqrt{3} \times \sqrt{3}$-(Pb,Sn) surface are shown in Fig. 1(a) for the filled states and (b) for the empty states. Observed spots in the STM images can be classified into three type of spots; white and gray (α), gray and white (β), and black and gray (γ), in the filled- and empty-state images, respectively. The arrangement of these spots are quite different from those observed in $\sqrt{3} \times \sqrt{3}$ mosaic phases, which consist of alternating chains of Pb (Sn) and Si adatoms [2,3]. The averaged number ratio of these spots α:β:γ is 42:52:6. Some atomic defects, which are seen as black spots in both the filled- and empty-state images, are also found on this surface. The average number ratio implies that the spots α and β corresponds to the adsorbates Sn and/or Pb and that the spots γ is due to a Si adatom. A local 3 × 3-(Pb,Sn) arrangement is also noticed on the $\sqrt{3} \times \sqrt{3}$-(Pb,Sn) surface. The number ratio α:β:γ in this 3 × 3 arrangement is 33:62:5. Although it is difficult to distinguish Pb and Sn only from these STM images, detailed comparison of corrugation pattern will give a reasonable identification of these spots as shown later. Corrugations along white lines in the STM images (a) and (b) are shown in Fig. 1 (c) and (d), respectively. The spot α is 0.03 ~ 0.05 nm higher than β in the filled state image and 0.02 ~ 0.04 nm lower in the empty state image. In order to determine the lateral position of the bright spots on the $\sqrt{3} \times \sqrt{3}$-(Pb,Sn) surface relative to the Si(111) substrate, STM images containing domain boundaries between the $\sqrt{3} \times \sqrt{3}$-(Pb,Sn) and 7 × 7 surfaces were obtained, as shown in Fig. 2. No steps are included in this STM image. Referring to the STM image of the 7 × 7 domain, we find that the all spots are located at the T4 site, which is the same position as those of Pb and Sn in the single adsorbate $\sqrt{3} \times \sqrt{3}$ surface [2,4].

The Pb 5*d* and Sn 4*d* core-level photoelectron spectra were measured for mosaic $\sqrt{3} \times \sqrt{3}$-Pb, $\sqrt{3} \times \sqrt{3}$-Pb, $\sqrt{3} \times \sqrt{3}$-(Pb,Sn), $\sqrt{3} \times \sqrt{3}$-Sn, and mosaic $\sqrt{3} \times \sqrt{3}$-Sn surfaces to investigate the chemical states of Pb and Sn adsorbates. Typical core-level PES spectra are shown in Fig. 3. As is seen in Fig. 3(b) and (d), the $\sqrt{3} \times \sqrt{3}$-Pb and $\sqrt{3} \times \sqrt{3}$-Sn surfaces show two major surface chemical shift components in the Pb 5*d* and Sn 4*d* core-level spectra, respectively. This is ascribable to charge density wave [10] or dynamical fluctuation of Sn adatoms between two different vertical positions above T4 site [11], which are detectable on PES but not in STM because of the *z* scale resolution limit and the difference in the probing time scale [12,13]. The peak positions and shape of Pb 5*d* and Sn 4*d* core-levels of the $\sqrt{3} \times \sqrt{3}$-(Pb,Sn) surface are similar to those of the $\sqrt{3} \times \sqrt{3}$-Pb and $\sqrt{3} \times \sqrt{3}$-Sn surfaces. This suggests that there is no specific charge transfer between Pb and Sn at the $\sqrt{3} \times \sqrt{3}$-(Pb,Sn) surface and that chemical states of Pb and

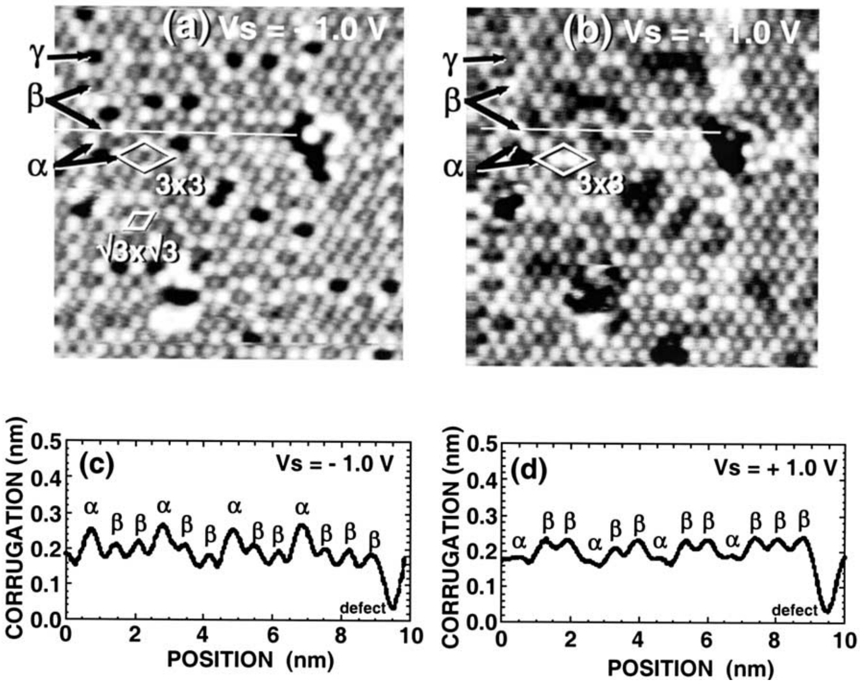

Fig. 1. STM images obtained from the $\sqrt{3} \times \sqrt{3}$-(Pb,Sn) surface at sample biases of −1.0 V (filled state) (a) and +1.0 V (empty state) (b). Spots are classified into three type of spots; white and gray (α), gray and white (β), and black and gray (γ) in the images (a) and (b), respectively. A $\sqrt{3} \times \sqrt{3}$ unit cell is indicated in the figure as well as 3 × 3 unit cell. Corrugations along white lines in the images (a) and (b) are also shown below.

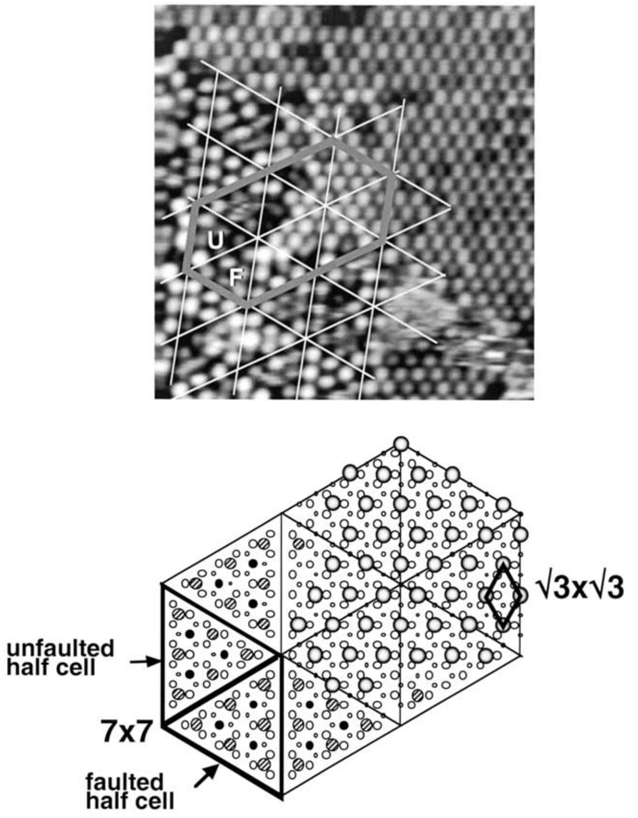

Fig. 2. STM images containing mixed domains of $\sqrt{3} \times \sqrt{3}$-(Pb,Sn) and 7 × 7 region at sample bias of −0.5 V. The schematic illustration of the area inside a hexagon drawn with gray solid lines is shown below.

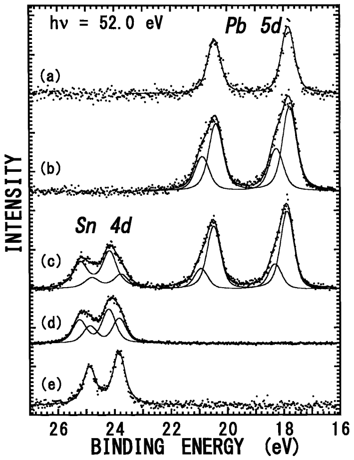

Fig. 3. Pb 5*d* and Sn 4*d* photoelectron spectra of mosaic $\sqrt{3} \times \sqrt{3}$-Pb surface with 1/6 ml Pb coverage (a), $\sqrt{3} \times \sqrt{3}$-Pb with 1/3 ml Pb coverage (b), $\sqrt{3} \times \sqrt{3}$-(Pb,Sn) (c), $\sqrt{3} \times \sqrt{3}$-Sn with 1/3 ml Sn coverage (d), and mosaic $\sqrt{3} \times \sqrt{3}$-Sn with 1/6 ml Sn coverage (e) after background subtraction. The solid lines show the components used to fit the spectra and resulting fit. A Gaussian width of 0.42 eV, a Lorentzian width of 0.28 eV, a spin-orbit split of 2.62 eV for Pb and 1.04 eV for Sn, a branching ratio of 0.80 for Pb and 0.67 for Sn, and a singularity index α of 0.00 were used for all components.

Sn are almost the same as those of the $\sqrt{3} \times \sqrt{3}$-Pb and $\sqrt{3} \times \sqrt{3}$-Sn surfaces. Since the minimum atomic distance between adsorbates in the $\sqrt{3} \times \sqrt{3}$ reconstruction at the coverage of 1/3 ml is 0.665 nm, it may be reasonable to have no direct interaction between Pb and Sn adsorbates.

On the other hand, the Pb 5*d* and Sn 4*d* core level spectra of the mosaic $\sqrt{3} \times \sqrt{3}$-Pb and mosaic $\sqrt{3} \times \sqrt{3}$-Sn surfaces show one major surface chemical shift component, respectively. The amounts of chemical shift of Pb 5*d* and Sn 4*d* spectra of mosaic $\sqrt{3} \times \sqrt{3}$-Pb and mosaic $\sqrt{3} \times \sqrt{3}$-Sn surfaces are similar to the component at lower binding energy of Pb 5*d* and Sn 4*d* spectra of $\sqrt{3} \times \sqrt{3}$-Pb and $\sqrt{3} \times \sqrt{3}$-Sn surfaces, respectively. This result well agrees with the result reported previously [11,12,14]. These results indicate that Pb and Sn atoms are stabilized at certain height or in one charged state on the mosaic $\sqrt{3} \times \sqrt{3}$ surfaces. These results also suggest that the Pb and Sn heights, or charged states, stabilized at the mosaic $\sqrt{3} \times \sqrt{3}$ surface are similar to those at the $\sqrt{3} \times \sqrt{3}$ surface.

Topographic STM images including domain boundary of the 7 × 7 and $\sqrt{3} \times \sqrt{3}$-Pb surfaces and that of the 7 × 7 and $\sqrt{3} \times \sqrt{3}$-Sn surfaces were observed to compare the height of the spots, as shown in Fig. 4. The 7 × 7 domains were included to supply a standard height for comparison. From these images, it is found that both Pb and Sn form only mosaic $\sqrt{3} \times \sqrt{3}$ phases, not $\sqrt{3} \times \sqrt{3}$ phases for the 1/3 ml coverage, at the regions next to the 7 × 7 domain. For the mosaic $\sqrt{3} \times \sqrt{3}$-Pb (-Sn) surface, it is reported that the STM images show clear different height contrast between Si and Pb (Sn) adatoms [3,14]; both the Pb and Sn adatoms are seen as brighter spots than Si adatom in the filled images. It is considered that the spots height at Pb (Sn) adatoms in the mosaic $\sqrt{3} \times \sqrt{3}$-Pb (-Sn) surface is similar to that in the $\sqrt{3} \times \sqrt{3}$-Pb (-Sn) surface, because the amount of chemical shift of Pb 5*d* (Sn 4*d*) spectrum of mosaic $\sqrt{3} \times \sqrt{3}$-Pb (-Sn) surface is similar to one of the two component of Pb 5*d* (Sn 4*d*) spectrum of $\sqrt{3} \times \sqrt{3}$-Pb surface, which is not distinguishable in the STM image. Corrugations along white lines drawn in Fig. 4 for the $\sqrt{3} \times \sqrt{3}$-Pb and $\sqrt{3} \times \sqrt{3}$-Sn surfaces are also compared with each other in Fig. 5. The Si adatoms in the mosaic $\sqrt{3} \times \sqrt{3}$ domains were 0.1 ~ 0.15 nm lower (darker) than those of Pb or Sn adatoms in the filled state images. The averaged spot heights at Sn are 0.03 ~ 0.05 nm higher than those at Pb in the filled state image, while they are 0.05 ~ 0.07 nm lower in the empty state image. This bias dependence of the corrugation of Pb and Sn is closely related to those of the spots α and β on the $\sqrt{3} \times \sqrt{3}$-(Pb,Sn) surface in Fig. 1. Thus, we conclude that Sn and Pb are located at α and β positions, respectively. Since Si adatoms are easily replaced with Pb and Sn in $\sqrt{3} \times \sqrt{3}$ surface and their STM images at the Si adatom position show black and gray spots in filled and empty state images, respectively [15], it is considered that Si adatoms are located at the γ position. Finally, we propose the local atomic arrangement of the 3 × 3-(Pb,Sn), as shown in Fig. 6. Then, the coverage of the local 3 × 3-(Pb,Sn) arrangement is determined to be 1/9 and 2/9 ml for Sn and Pb, respectively.

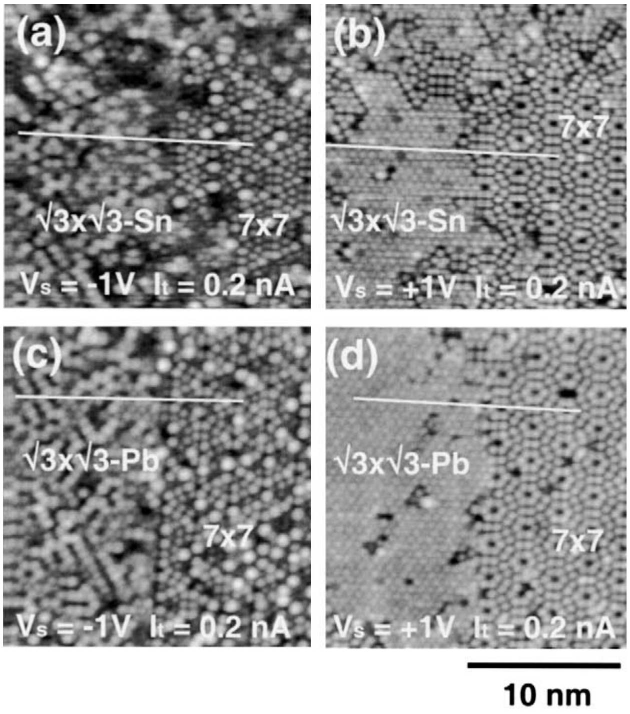

Fig. 4. STM images of mixed domains of $\sqrt{3} \times \sqrt{3}$-Pb and 7 × 7 at sample biases of −1.0 V (a) and +1.0 V (b), and those of $\sqrt{3} \times \sqrt{3}$-Sn and 7 × 7 at sample biases of −1.0 V (c) and +1.0 V (d).

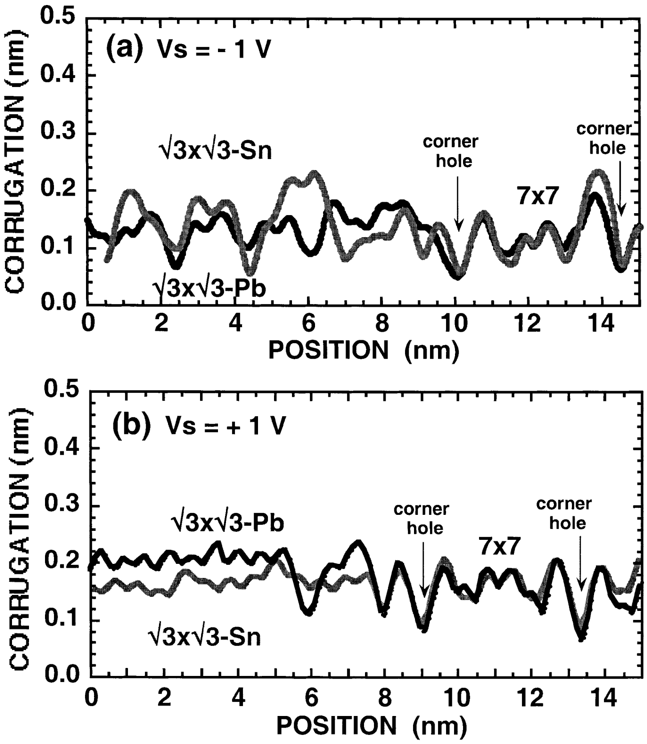

Fig. 5. Corrugations of the domains of $\sqrt{3} \times \sqrt{3}$-Pb (black lines) and $\sqrt{3} \times \sqrt{3}$-Sn (gray lines) are shown along white lines drawn in Fig. 4, including the 7 × 7 domains for comparison. (a) the filled state image (b) the empty state image.

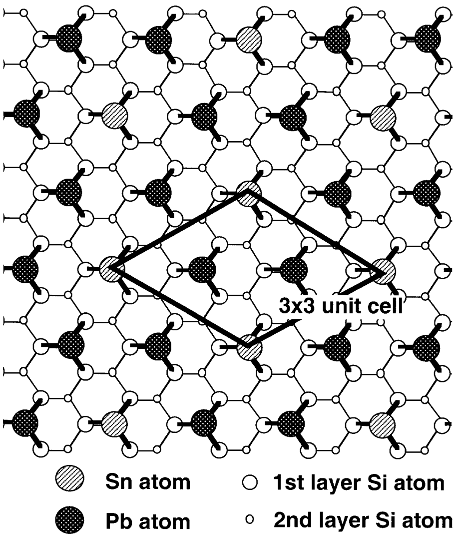

Fig. 6. The schematic illustration of the local atomic arrangement of the 3×3-(Pb,Sn) surface.

So far, Schmid et al. have firstly reported that STM shows clear discrimination of two chemical species in a metal alloy surface [16]. This is the first time on silicon surface that two foreign metal adsorbates are distinguished by STM. Since the heights of adsorbates from the Si first layer at the $\sqrt{3} \times \sqrt{3}$ surface are reported to be 0.13 ± 0.05 nm for Pb [17] and 0.23 ± 0.03 nm for Sn [18], respectively, it is interesting to examine the heights of Sn and Pb at the $\sqrt{3} \times \sqrt{3}$-(Pb,Sn) surface to compare single adsorbate with binary adsorbate. To determine the heights of Pb and Sn at the $\sqrt{3} \times \sqrt{3}$-(Pb,Sn) surface, and it will be helpful to use co-axial impact collision ion scattering spectroscopy (CAICISS).

4. Conclusion

The $\sqrt{3} \times \sqrt{3}$-(Pb,Sn) surface was studied by STM and core-level PES. The STM images at filled and empty states were mainly classified into three types of spots and all spots were located at the T4 site. Bias dependence of local height contrasts was compared between the $\sqrt{3} \times \sqrt{3}$-(Pb,Sn), the $\sqrt{3} \times \sqrt{3}$-Pb, and the $\sqrt{3} \times \sqrt{3}$-Sn surfaces. From core-level PES, it was found that there was no specific charge transfer between Pb and Sn and that the chemical bonding state of Pb and Sn on the $\sqrt{3} \times \sqrt{3}$-(Pb,Sn) surface was almost the same as those on the $\sqrt{3} \times \sqrt{3}$-Pb and $\sqrt{3} \times \sqrt{3}$-Sn surfaces. Local electronic structures (heights) at the Pb and Sn positions were compared with each other in the STM images of a mixed domain of the 7×7 and $\sqrt{3} \times \sqrt{3}$-Pb ($\sqrt{3} \times \sqrt{3}$-Sn) surfaces. From these results, atomic species on the STM image of the $\sqrt{3} \times \sqrt{3}$-(Pb,Sn) surface was identified. It was also shown that the $\sqrt{3} \times \sqrt{3}$-(Pb,Sn) surface had the local 3×3 reconstruction.

References

[1] R.W. Olesinki, G.J. Abbaschian, Bull. Alloy Phase Diagrams 5 (1984) 271.
[2] E. Ganz, I.-S. Hwang, F. Xiong, S.K. Theiss, J. Golovchenko, Surf. Sci. 257 (1991) 259.
[3] C. Törnevik, M. Göthelid, M. Hammar, U.O. Karlsson, N.G. Nilsson, S.A. Flodstrom, C. Wigren, M. Ostling, Surf. Sci. 314 (1994) 179.
[4] J. Nogami, S.-I. Park, C.F. Quate, J. Vac. Sci. Technol. A7 (1989) 1919.
[5] J. Yuhara, K. Matsuda, Y. Hattori, K. Morita, Appl. Surf. Sci. 162–163 (2000) 368.
[6] J. Yuhara, K. Soda, K. Morita, Surf. Sci. 482–485 (2001) 32.
[7] D. Nakamura, J. Yuhara, K. Morita, Appl. Surf. Sci. 130–132 (1998) 72.
[8] D. Nakamura, J. Yuhara, K. Morita, Nucl. Instrum. Methods B157 (1999) 279.
[9] J. Yuhara, D. Nakamura, K. Soda, K. Morita, Surf. Sci. 482–485 (2001) 1374.
[10] T.E. Kidd, T. Miller, T.-C. Chiang, Phys. Rev. Lett. 83 (1999) 2789.
[11] J. Avila, A. Mascaraque, E.G. Michel, M.C. Asensio, G. Le Lay, J. Ortega, R. Perez, F. Flores, Phys. Rev. Lett. 82 (1999) 442.
[12] M. Göthelid, M. Björkqvist, E.G. Michel, M.C. Asensio, G. Le Lay, C.J. Karlsson, Phys. Rev. B52 (1995) 14532.
[13] R.I.G. Uhrberg, H.M. Zhang, T. Balasubramanian, S.T. Jemander, N. Lin, G.V. Hansson, Phys. Rev. B62 (2000) 8082.
[14] R.I.G. Uhrberg, H.M. Zhang, T. Balasubramanian, Phys. Rev. Lett. 85 (2000) 1036.
[15] J.M. Gomez-Rodriguez, J.-Y. Veuillen, R.C. Cinti, Surf. Sci. 377–379 (1997) 45.
[16] M. Schmid, H. Stadler, P. Varga, Phys. Rev. Lett. 70 (1993) 1441.
[17] J.M. Roesler, M.T. Sieger, T. Miller, T.-C. Chiang, Surf. Sci. 329 (1995) L588.
[18] T. Yamanaka, S. Ino, Phys. Rev. B61 (2000) R5074.